W. GĘBAROWSKI*, S. PIETRZYK*

GROWTH CHARACTERISTICS OF THE OXIDE LAYER ON ALUMINIUM IN THE PROCESS OF PLASMA ELECTROLYTIC OXIDATION

CHARAKTERYSTYKA WZROSTU WARSTWY TLENKOWEJ NA ALUMINIUM W PROCESIE PLAZMOWEGO UTLENIANIA ELEKTROLITYCZNEGO

During the formation of the oxide layer by plasma electrolytic oxidation (PEO), the electrochemical processes are accompanied by the plasma micro-discharges, occurring uniformly over the coated electrode. Application of an alternating current with strictly controlled electrical parameters can affect the character of the discharges, and consequently the properties of the obtained layers. When the cathodic current density exceeds anodic, at some point, a sudden change in the appearance of micro-discharges and a decrease in the intensity of the acoustic emission can be observed – in literature this effect is called "soft sparking". In the present work, the evolution of the electrical properties of the layers at various stages of their formation has been characterized, using electrochemical impedance spectroscopy. The study showed a significant decrease in charge transfer resistance and increase in capacitance of the oxide layer after reaching the "soft sparking". This indicates a significant change in the structure of the oxide layer, in the barrier and main part, which is additionally confirmed by measuring the breakdown voltage.

Keywords: Plasma electrolytic oxidation, PEO, aluminium oxide, 'soft sparking'

Podczas formowania warstewki tlenkowej metodą plazmowego utleniania elektrolitycznego (PEO), procesom elektrochemicznym towarzyszą mikro-wyładowania plazmowe, występujące równomiernie na pokrywanej elektrodzie. Zastosowanie prądu zmiennego, o ściśle kontrolowanych parametrach, pozwala wpływać na charakter wyładowań i w konsekwencji na właściwości otrzymywanych warstw. W przypadku, kiedy gęstość prądu katodowego jest wyższa od anodowego, na pewnym jego etapie, można zaobserwować nagłą zmianę postaci wyładowań oraz spadek natężenia emisji akustycznej, co w literaturze nazywane jest tzw. "miękkim iskrzeniem". W niniejszej pracy została scharakteryzowana ewolucja właściwości elektrycznych warstwy tlenkowej na poszczególnych etapach jej formowania, za pomocą elektrochemicznej spektroskopii impedancyjnej. Przeprowadzone badania pokazały znaczny spadek oporu przeniesienia ładunku oraz wzrost pojemności elektrycznej warstwy po osiągnięciu stanu "miękkiego iskrzenia". Wskazuje to na duże zmiany zachodzące w strukturze warstwy tlenkowej, w jej części barierowej oraz właściwej, co dodatkowo potwierdzają pomiary napięcia przebicia.

1. Introduction

Plasma Electrolytic Oxidation (PEO) is a process of forming oxide layers on Al, Ti and Mg alloys. It is based on the anodic oxidation in aqueous solutions and on the application of voltage exceeding the breakdown voltage of the developing oxide layer on the surface of metal [1-3]. This results in an occurrence of short-living electrical micro-discharges, uniform on the whole surface of the electrode, which promotes growth of oxide layer. These plasma discharges locally heat up the oxide to high temperature (~10 000K) and cause the fusing of the oxide and the substrate material which are ejected towards oxide/electrolyte interface in high electric field through discharge channels [4,5]. Due to the low magnitude of an individual discharge, very high temperature gradient (electrolyte has room temperature) causes rapid solidifying of melted material and its depositing on and within oxide layer. These processes are mainly responsible for the characteristic structure and morphology of oxide layers obtained in PEO which have high microhardness, wear and corrosion resistance [6,7].

Besides the composition of electrolyte, electrical conditions are the main factors influencing the PEO process. Oxidation can be conducted using direct, alternate and pulsed current [1,2]. Recently, most researches in PEO are based on AC and pulsed techniques which effectively eliminate main disadvantages of DC – preferential and destructive large discharges in later stages of the process [2,8]. Initially, AC sources are based on mains frequency and characterized by simple construction but very limited possibility of control. At present, the AC techniques are allowing to use various kinds of waveforms, frequency and duty cycles or more complex positive and negative pulses sequences in case of the pulsed power supplies [1]. There are only few papers which describe so called 'soft sparking' phenomenon which takes place when

*   AGH UNIVERSITY OF SCIENCE AND TECHNOLOGY, FACULTY OF NON-FERROUS METALS, AL. A. MICKIEWICZA 30, 30-059 KRAKÓW, POLAND

negative charge (cathodic) overcomes the positive one (anodic) during one period under the AC condition [9-17]. The transition to the 'soft sparking' discharges appears at certain time of the process and it is connected with the decrease of the anodic voltage, significant reduction of the acoustic emission and change of the discharges appearance, also observed in optical emission spectrum [18,19]. During the 'soft sparking', the higher growth rate of oxide layer is noticed as well as higher process yield [10]. The higher cathodic current with respect to the anodic one causes the sooner occurrence of the transition to 'soft sparking' [17].

According to literature [20, 21], the cathodic current during the PEO processes have following roles: interrupting of the micro-discharges, cooling and refreshing of electrolyte near the electrode surfaces.

Sah et al. [16] claimed the cathodic pulses randomize places of the following anodic breakdowns due to the formation of high resistive porous oxide layer in places of discharges. This layer prevents from the occurrence of a next breakdown in the same place, but it is not clear enough what reactions of forming anodic film are driven by the cathodic current flow. Moreover experiments were conducted at the beginning stage of the oxidation process where the oxide layer is very thin and it may be not representative for the whole process.

The effect of the 'soft sparking' was observed not only for aluminium alloys but also for Mg alloy [22].

Because of no evident explanation of the cause of the transition to the 'soft sparking' during PEO process, more profound studies about this phenomenon are required to shed more light on the mechanisms. This paper is presented to give more information about changes in electrical properties, structure and morphology of the oxide layer during process time, especially before and after the 'soft sparking' transitions.

2. Experimental

The samples of size $10\times30\times1.5$ mm were made of 1050 aluminium alloy. Before the PEO process, the samples were prepared in the following steps: degreasing in acetone, etching in 0.25 mol·dm^{-3}NaOH solution, brightening in 7 mol·dm^{-3}HNO$_3$ solution and rinsing in distilled water. Oxidation of samples was conducted in 4 dm^3 stainless steel tank which acted as counter electrode. Composition of electrolyte was: 0.04 mol·dm^{-3} KOH, 0.08 mol·dm^{-3} Na$_2$SiO$_3$ and its temperature was maintained at 22±1°C. The bath was agitated by mechanical stirrer. PEO process was conducted using AC 100Hz square waveform with 0.5 ms dead time between each half-period. Average current densities of positive (anodic) and negative (cathodic) half-periods were set at 10 A·dm^{-2} and 12.5 A·dm^{-2} respectively. The only variable parameter was the time of the process, which was up to 60 min in steps of 10 min.

After the PEO process, the samples were rinsed in distilled water in an ultrasonic cleaner in order to remove residual electrolyte from the pores of oxide layers. Then the samples were put into 0.1 mol·dm^{-3} Na$_2$SO$_4$ and after 30 min when the semi steady state was reached (stable OCP), impedance measurements were performed on potentiostat Autolab PG-

STAT302N with FRA2 module. The measurement glass vessel was 150 cm^3 and the counter electrode was high purity graphite rod. The excitation signal was 10 mV sine wave with respect to OCP and frequency range 1 MHz to 50 mHz. Equivalent circuit of system was fitted using ZView software.

The breakdown voltages and current response in cathodic ranges were determined by polarization samples with oxide coatings (on another series of samples) in high range of potentials. The scan speed was 3 V· s^{-1} (up to 600 V) and 1 V·s^{-1} (up to tens of volts) for anodic and cathodic direction respectively. Measurements were conducted in the base electrolyte, using programmable DC power supply Chroma 62012P.

Phase composition was determined by X-ray diffraction on top surfaces of layers (Rigaku MiniFlex). Observations and elemental analysis (EDX) of the top surfaces and cross-sections of layers were conducted on SEM (Hitachi SU-70). Chemical composition was calculated from K lines of standardless analysis.

3. Results and discussion

Figure 1 presents the changes of the anodic and cathodic voltage, the mass of samples and the thickness of the oxide layer during the experiments. The cathode current density is higher than anodic, nevertheless cathodic voltage is significantly lower than anodic one (80:420V). This proves that cathodic reactions proceed much faster than anodic. This is due to higher mobility of hydrogen ions through the oxide than ions containing oxygen. On the voltage curves it can be distinguished following stages of the process. At the beginning, voltage linearly increases very fast up to about 400V. It is related to the forming of dielectric barrier oxide layer on the metal surface.
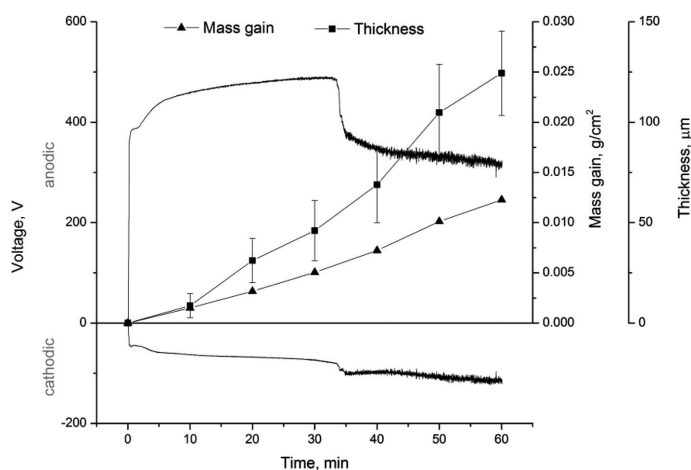

Fig. 1. Voltage, mass and thickness changes during oxidation

At certain value of voltage this layer starts to be broken down by high electric field. Then the voltage stops increasing and holds on almost the same level by next 30 minutes of the process. During this time, the number of micro-discharges decreases gradually and they become larger and last longer. In 33rd minute, rapid drop of anodic voltage takes place, which is connected with the transition to the 'soft sparking'. The cathodic voltage almost does not change. Despite the considerable changes in the process, no changes in rate of mass gain

are observed. Slight increase of growth speed indicates that oxide layer becomes more porous, hence has lower density. It means that the electrode mass changes are proportional only to the flowing charge, in accordance with the Faraday's law, and are not being changed by physical processes. However, the drop of anodic voltage (from about 480 to 370 V) at the constant current causes reduction of power consumption of about 23 %.
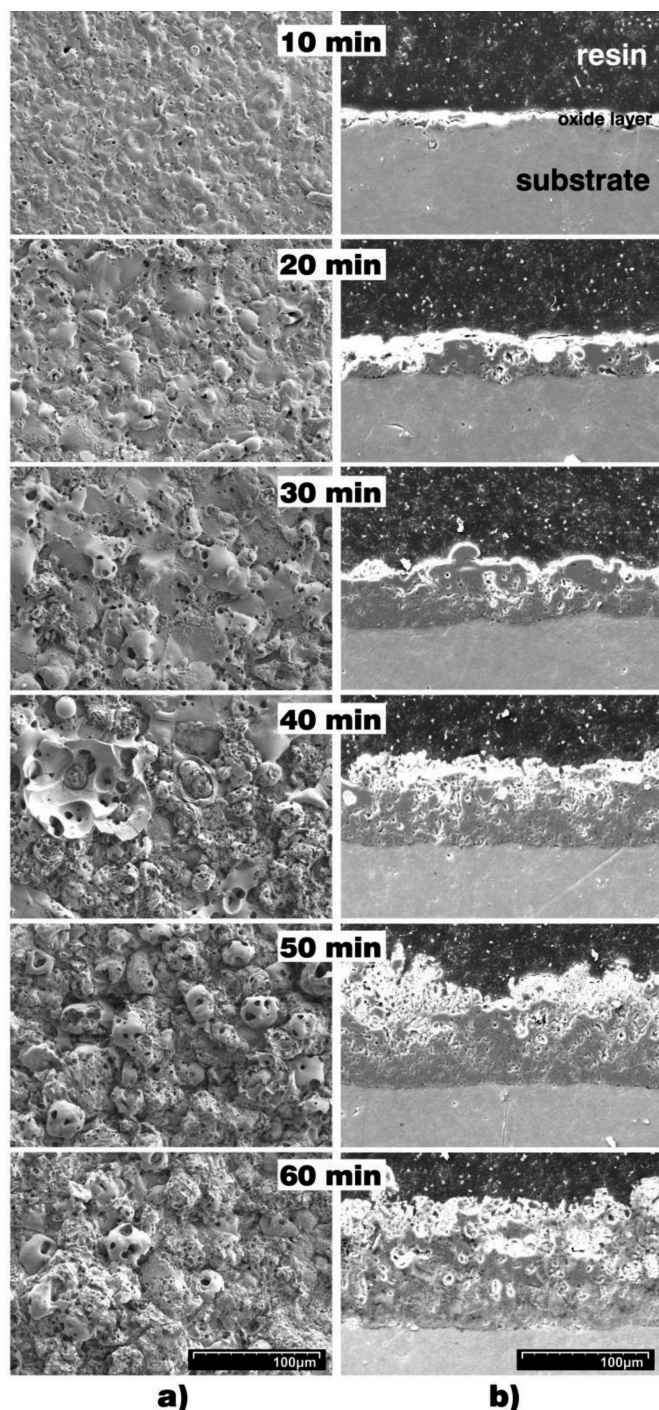

Fig. 2. SEM microphotographs of surface (a) and cross-section (b) of oxide layers

SEM microphotographs presented in Fig. 2 show evolution of the layer structure during process. It is visible that after the 'soft sparking' transition, the oxide layer surface is rougher and much more developed. Macroscopic observations

of layers surfaces show that before the 'soft sparking' transition, darker and lighter areas can be distinguished. With the process time, lighter areas become larger and finally cover the entire surface of the electrode. These lighter areas correspond to the high developed precipitations on the surface. Thus, the 'soft sparking' transition starts after the whole surface of oxide layer is covered by these precipitations. This corresponds with Matykina et al. [15] who suggested that oxide layer must have sufficient thickness to change micro-discharge regimes. The cathodic current causes changes in the structure of the oxide layer, probably mainly by hydrogen evolution, and allows the presence of the 'soft sparking'. This state is supported by the fact that at higher cathodic current, the transition to the 'soft sparking' occurs sooner [17]. Therefore, the pass of a certain amount of charge (cathodic) is needed in order to make appropriate changes in oxide layer. EDX and XRD analysis of oxide surface (Fig. 3) indicate that after the 'soft sparking' transition, concentration of silicon (mullite phase) is decreasing with oxidation time and concentration of electrolyte components – K and Na – is increasing.
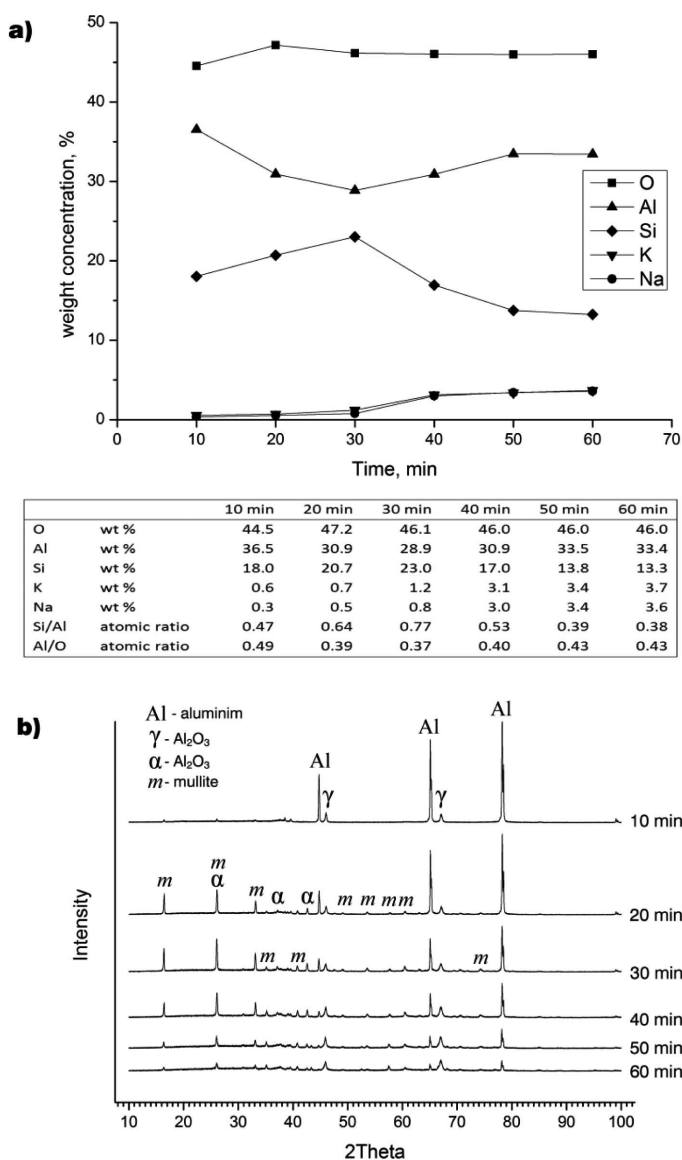

		10 min	20 min	30 min	40 min	50 min	60 min
O	wt %	44.5	47.2	46.1	46.0	46.0	46.0
Al	wt %	36.5	30.9	28.9	30.9	33.5	33.4
Si	wt %	18.0	20.7	23.0	17.0	13.8	13.3
K	wt %	0.6	0.7	1.2	3.1	3.4	3.7
Na	wt %	0.3	0.5	0.8	3.0	3.4	3.6
Si/Al	atomic ratio	0.47	0.64	0.77	0.53	0.39	0.38
Al/O	atomic ratio	0.49	0.39	0.37	0.40	0.43	0.43

Fig. 3. XRF (a) and XRD (b) analysis of oxide layers surfaces
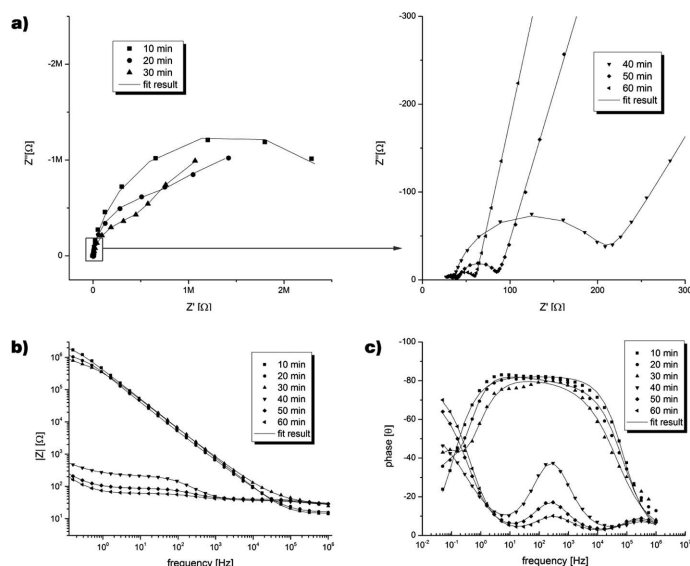
410

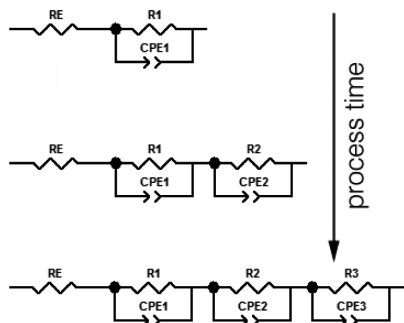Fig. 4. EIS measurements: a) Nyquist plot, b) Bode plot – impedance modulus, c) Bode plot – phase shift

Fig. 5. The proposed equivalent circuits of oxide coatings and their development during the process time

the 'soft sparking' was established, oxide layer resistance for charge transfer (R_1) drops for several orders of magnitude. Two time-constant can be found at high frequencies indicating two-stage mechanism of charge transfer. Moreover, the oxide layer increases its capacitance which is connected with the increase of the surface development and layer thickness. These changes during oxidation may indicate that evolution of hydrogen destroys the barrier layer by forming some defects in its continuity, which facilitates passing of charge and mass towards metal/oxide interface during anodic cycle. Figure 5 shows the evolution of equivalent electrical circuits of the oxide layer. The values of elements used to fit experimental results are presented in Table 1.
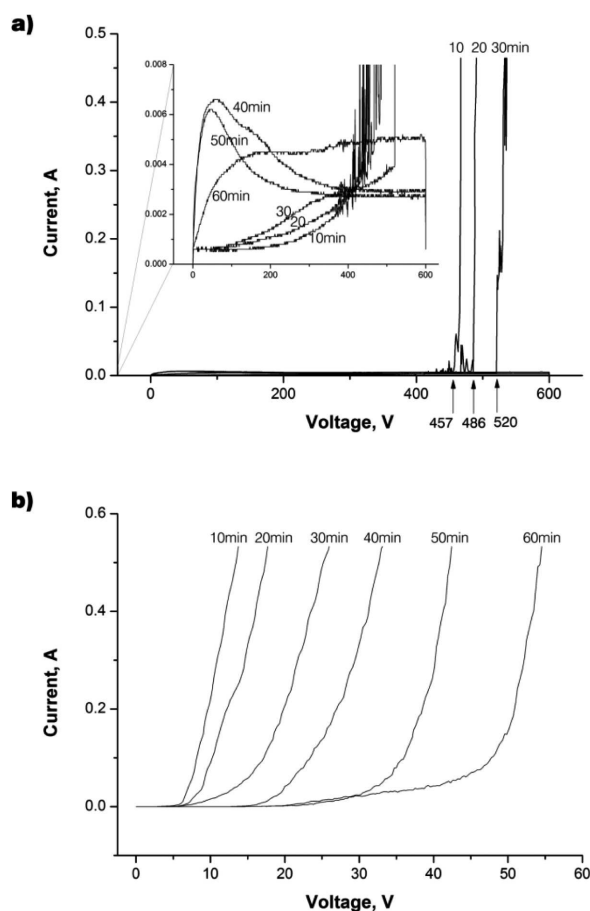

Fig. 6. Wide range polarisations of the samples in anodic (a) and cathodic (b) direction

Experiments with linear polarization of coated electrodes, in anodic and cathodic direction, in high range of potentials give quite interesting results (Fig. 5). In case of samples after 10, 20 and 30 min of oxidation (before the 'soft sparking') at potentials 457, 486 and 520 V respectively, the oxide layer was broken down by electrical discharges and current started to flow. These potentials correspond to breakdown or critical voltages. In case of samples near the 'soft sparking' transition, higher current started to flow but breakdown voltage was not reached (in range up to 600 V). For samples after 40 and 50 min of oxidation, the current reached the maximum value, then decreased, thus it behaves like negative resistance. It is probably due to the passivation of active regions (defects) in the barrier layer through 'sealing' them by the formation of oxide. For sample after 60 min of oxidation, current was not

TABLE 1

Values of elements for fitted circuits

	10 min	20 min	30 min	40 min	50 min	60 min
Re [Ω]	14.43	15.6	22.5	25.1	27	24.8
R_1 [Ω]	2.88E+06	5.66E+05	5.35E+05	10.86	13.44	13.22
CPE_1 [F]	4.42E-07	6.91E-07	6.16E-07	1.97E-06	6.26E-07	1.74E-06
n_1	0.91	1	0.89	0.75	0.83	0.74
R_2 [Ω]		2.86E+06	2.78E+06	1.68E+02	46.01	22.50
CPE_2		1.62E-06	2.32E-06	2.24E-05	6.18E-05	1.25E-04
n_2		0.82	0.91	0.87	0.84	0.81
R_3 [Ω]			(1E+20)	(1E+20)	(1E+20)	(1E+20)
CPE_3 [F]			2.90E-03	2.99E-03	5.94E-03	7.18E-03
n_3			0.17	0.66	0.81	0.86
X^2 sum	0.075	0.078	0.059	0.004	0.002	0.001

The electrochemical impedance spectroscopy measurements (Fig. 4) show a significant change in electrical properties of the oxide coating at the 'soft sparking' transition. After 10 minutes of oxidation, coating has very high resistance (order of mega ohms) for charge and mass transfer. With the process time, coating becomes less resistive and second time-constant becomes more evident. After 40 min when

decreasing with the increase of voltage. In case of the cathodic polarisation (Fig. 5b), the higher process time, the higher voltage is needed to initiate high current flow due to higher barrier for hydrogen evolution.

Another observation is that when the 'soft sparking' during the PEO is established, it is possible to change electrical parameters in wide ranges, such as frequency, duty cycles or overall current densities without losing this effect. Only one condition has to be fulfilled: the cathodic charge must exceed the anodic charge in each period.

The presented assumptions have to be confirmed by further corrosion and mechanical tests (especially adhesion) of the oxide layers. This will help to determine the usefulness of the 'soft sparking' in practical application.

4. Conclusions

The results presented in this work show how significant changes occur in the electrical properties of oxide layer during the 'soft sparking' transitions. The considerable drop of charge transfer resistance is most likely due to barrier layer corrosion caused by hydrogen evolution during the cathodic cycle. The structure changes can also be enhanced by greater chemical dissolution of the oxide by the electrolyte alkalized near to the oxide interface (by reduction of hydrogen ions). Additionally, higher electrical capacitance of the coating results in larger charge accumulated in the oxide layer.

In summary, the cathodic current induces the two independent effects. One is the transformation of the oxide layer that allows occurring of the 'soft sparking'. The second is sustaining the 'soft sparking' by creating a particular distribution (not yet defined) of charge and components of electrolyte near the metal/oxide and the oxide/electrolyte interfaces.

REFERENCES

[1] B.L. Jiang, Y.M. Wang, Plasma electrolytic oxidation treatment of aluminium and titanium alloys in: Hanshan Dong (Ed.), Surface Engineering of light alloys, Woodhead (2010).

[2] A. Yerokhin, X. Nie, A. Leyland, A. Matthews, S.J. Dowey, Surf. Coat. Tech. **122**, 73 (1999).

[3] M. Aliofkhazraei, A.S. Rouhaghdam, Fabrication of nanostructures by plasma electrolysis, Weinheim 2010.

[4] L. Snizhko, A.L. Yerokhin, A. Pilkington, N. Gurevina, D.O. Misnyankin, A. Leyland, A. Matthews, Electrochim. Acta **49**, 2085 (2004).

[5] C.S. Dunleavy, I.O. Golosnoy, J.A. Curran, T.W. Clyne, Surf. Coat. Tech. **203**, 3410 (2009).

[6] A. Yerokhin, A. Shatrov, V. Samsonov, P. Shashkov, A. Pilkington, A. Leyland, A. Matthews, Surf. Coat. Tech. **199**, 150 (2005).

[7] L. Wen, Y. Wang, Y. Zhou, J.-H. Ouyang, L. Guo, D. Jia, Corros. Sci. **52**, 2687 (2010).

[8] S. Xin, L. Song, R. Zhao, X. Hu, Thin Solid Films **515**, 326 (2006).

[9] A.S. Shatrov, V.I. Samsonov, Patent US 2003/0188972 A1.

[10] F. Jaspard-Mecuson, T. Czerwiec, G. Henrion, T. Belmonte, L. Dujardin, A. Viola, J. Beauvir, Surf. Coat. Tech. **201**, 8677 (2007).

[11] A.I. Slonova, O.P. Terleeva, Prot. Met. **44**, 65 (2011).

[12] E. Matykina, R. Arrabal, A. Mohamed, P. Skeldon, G.E. Thompson, Corros. Sci. **51**, 2897 (2009).

[13] E. Matykina, R. Arrabal, P. Skeldon, G.E. Thompson, Surf. Interface Anal. **42**, 221 (2010).

[14] E. Matykina, R. Arrabal, P. Skeldon, G.E. Thompson, Electrochim. Acta **54**, 6767 (2009).

[15] E. Matykina, R. Arrabal, P. Skeldon, G.E. Thompson, P. Belenguer, Surf. Coat. Tech. **205**, 1668 (2010).

[16] S.P. Sah, Y. Tatsuno, Y. Aoki, H. Habazaki, Corros. Sci. **53**, 1838 (2011).

[17] W. Gębarowski, S. Pietrzyk, Arch. Metall. Mater. **58**, 241 (2013).

[18] M.D. Klapkiv, H.M. Nykyforchyn, V.M. Posuvailo, Mater. Sci. **30**, 333 (1994).

[19] R. Arrabal, E. Matykina, T. Hashimoto, P. Skeldon, G.E. Thompson, Surf. Coat. Tech. **203**, 2207 (2009).

[20] S. Xin, L. Song, R. Zhao, X. Hu, Thin Solid Films **515**, 326 (2006).

[21] M. Chen, Y. Ma, Y. Hao, Front. Mech. Eng. China **5**, 98 (2009).

[22] R. Arrabal, E. Matykina, T. Hashimoto, P. Skeldon, G.E. Thompson, Surf. Coat. Tech. **203**, 2207 (2009).